ELSEVIER

Catalysis Today 35 (1997) 369–377

CATALYSIS TODAY

Combined infrared and mass spectrometric study of reactions of adsorbed NO and CO on 0.5 wt% Rh/SiO_2 catalyst

Steven S.C. Chuang *, Cher-Dip Tan

Department of Chemical Engineering, The University of Akron, Akron, OH 44325-3906, USA

Abstract

NO adsorption, CO adsorption, NO temperature-programmed desorption and decomposition (TPD), and temperature-programmed reaction (TPR) of NO–CO have been studied over 0.5 wt% Rh/SiO_2 catalysts by a combined infrared and mass spectrometric technique. Infrared study reveals that the high wavenumber $Rh–NO^{\delta-}$ at 1723–1740 cm^{-1} is the dominant adsorbate during TPD and TPR with NO:CO = 1:1. During TPR, CO reduces part of Rh surface resulting in the formation of the low wavenumber $Rh–NO^{\delta-}$ at 1634–1680 cm^{-1}. Increasing CO partial pressure (i) promotes the formation of Rh^0 sites, producing linear CO, (ii) increases the selectivity to N_2O below the light-off temperature, (iii) raises the light-off temperature, and (iv) promotes the formation of Si–NCO and Rh–NCO. Comparison of results of the present study with those of previous studies on 4 wt% Rh/SiO_2 shows that different dispersion of Rh crystallites on SiO_2 support results in significant variation in chemisorptive and reactive properties of Rh metal for the NO–CO reaction.

Keywords: Infrared spectroscopy; Mass spectroscopy; Rh/SiO_2 catalyst

1. Introduction

In situ infrared (IR) spectroscopy has been widely used to study adsorbates on supported metal catalysts [1–7]. Infrared spectroscopy provides unique information on both properties of adsorbates and characteristics (i.e. oxidation state and geometric structure) of the surface sites that chemisorb adsorbates. Depending on the specific reaction conditions, adsorbates may follow various pathways: (i) desorbing to the gas phase and returning to its initial reactant form, (ii) surface reactions leading to the formation of both desired and side products, and (iii) residing on the surface and remaining inactive. Identification of the fate of an adsorbate requires simultaneous measurements of variation in concentration of adsorbates as well as that of gaseous reactants and products under transient conditions [1,7,8]. One effective approach for such measurements is a combined IR and mass spectrometric (MS) technique in which in situ IR spectroscopy measures the concentration of adsorbates and MS determines the concentration of the gaseous species resulting from interactions and reactions of the adsorbates.

Both IR and MS have been widely used in catalysis research. These techniques have often been used separately, resulting in the difficulty in correlating IR with MS results. Few studies using the combined IR and MS technique have been reported. An earlier combined IR-MS study of NO and CO adsorption on a 4 wt% Rh/SiO_2 catalyst with Rh crystallite size of 63 Å re-

* Corresponding author.

0920-5861/97/$17.00 Copyright © 1997 Elsevier Science B.V. All rights reserved.
PII S0920-5861(96)00216-7

vealed that exposure of linear and gem-dicarbonyl CO to gaseous NO leads to desorption of both forms of adsorbed CO and adsorption of NO as Rh–$NO^{\delta-}$ and Rh–$NO^{\delta+}$ in the 298–413 K temperature range [9]. Transient IR-MS study also showed that adsorbed $NO^{\delta-}$ on the surface of Rh crystallite is an active precursor for NO dissociation [10]. Due to the significant difference in Rh loading and dispersion between 4 wt% Rh/SiO_2 and a three-way Pt–Rh automobile catalyst, results obtained from 4 wt% Rh/SiO_2 may not be directly relevant to the behavior of adsorbates on the surface of the three-way catalyst.

The objective of this study is to determine the reaction pathways of adsorbed NO during temperature-programmed desorption, decomposition, and reaction with CO on 0.5 wt% Rh/SiO_2. 0.5 wt% Rh/SiO_2 contains highly dispersed Rh crystallite of which dispersion resembles that of Rh on the typical three-way catalyst. Results of this study are compared with those of 4 wt% Rh/SiO_2 [8–10] and other results described in the literature to shed light on the behavior of adsorbed NO on the highly dispersed Rh catalysts under reaction conditions.

2. Experimental

The catalyst used in this study was a 0.5 wt% Rh/SiO_2 which was prepared by incipient wetness impregnation of large pore (Stream, 300 $m^2\ g^{-1}$) SiO_2 support with $RhCl_3 \cdot 3H_2O$ (Alfa Chemicals) solution. The ratio of the volume of solution to the weight of support material used for the catalyst was 1 cm^3 to 1 g. After impregnation, the catalyst sample was dried overnight in air at 303 K and reduced in flowing H_2 at 673 K for 16 h. The catalyst was pressed into a thin disk and placed in an in situ IR reactor cell capable of operating up to 873 K and 6 MPa. The details of the in situ IR reactor cell, experimental apparatus, and procedures have been reported elsewhere [8]. The catalyst in the IR cell was further reduced with H_2 at 673 K for 2 h prior to initiating the reaction study. The reaction mixture consisted of CO (Commercial grade), NO (UHP), and He (UHP) which were controlled by mass flow controllers.

Temperature-programmed desorption (TPD) of adsorbed NO was carried out at a heating rate of 15 K min^{-1} in flowing helium at 30 $cm^3\ min^{-1}$; temperature-programmed reaction of NO–CO was studied at a heating rate of 15 K min^{-1} with a mixture of NO:CO:He = 10:10:30 $cm^3\ min^{-1}$ and NO:CO:He = 5:50:30 $cm^3\ min^{-1}$. The change in concentration of adsorbates was monitored by an FT-IR spectrometer with a resolution of 4 cm^{-1}; the effluent from the IR reactor cell was monitored continuously using a Balzers QMG 112 quadrupole mass spectrometer (MS). The mass-to-charge (m/e) ratios monitored were 28 for CO and N_2, 30 for NO, and 44 for both N_2O and CO_2.

3. Results and discussion

Fig. 1 shows the infrared spectra of adsorbed NO at 303 K and 0.1 MPa during temperature-

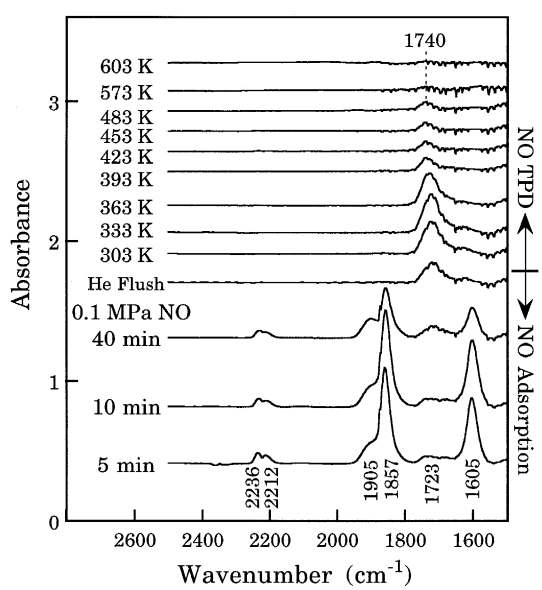

Fig. 1. IR spectra of NO adsorption at 303 K and 0.1 MPa followed by temperature-programmed desorption on 0.5 wt% Rh/SiO_2.

programmed desorption and decomposition. Exposure of Rh/SiO_2 catalyst to 0.1 MPa of NO at 303 K in a batch mode produced gaseous N_2O bands at 2236 and 2212 cm^{-1}, weakly adsorbed NO on SiO_2 at 1857 and 1605 cm^{-1}, and adsorbed NO on Rh at 1723 cm^{-1}. The 1723 cm^{-1} band may be assigned to a high wavenumber $Rh–NO^{\delta-}$ which will be further discussed. Prolonged exposure of the catalyst to gaseous NO led to the growth of the band at 1723 cm^{-1} and decrease in the IR intensity of weakly adsorbed NO on SiO_2. Gaseous N_2O and weakly adsorbed NO were removed by flowing helium while the $Rh–NO^{\delta-}$ band continued to increase in intensity.

Fig. 1 also shows that temperature-programmed desorption of adsorbed NO caused a decrease in the $Rh–NO^{\delta-}$ intensity and an upward shift from 1723 cm^{-1} at 303 K to 1740 cm^{-1} at 483 K. Closer examination reveals that the bands in 1723–1740 cm^{-1} region consist of at least two bands. These bands are centered about 1740 cm^{-1} at temperatures above 423 K and around 1723 cm^{-1} at temperatures below 423 K. The change in wavenumber of the $Rh–NO^{\delta-}$ from 1723 cm^{-1} to 1740 cm^{-1} appears to be a function of temperature where one form of $Rh–NO^{\delta-}$ converts to another with an increase in temperature. Clear distinction between these two bands is not possible; the difference in structure between the species contributing these two bands cannot be determined.

Assignment of the structure of adsorbed NO on the surface of Rh single crystal and supported Rh catalysts has been based on the presumed analogy in vibrational frequency between adsorbed NO on the metal surface and nitrosyl metal complex. Table 1 summarizes the similarities and the differences in vibrational frequencies of adsorbed NO on the surface of Rh/SiO_2, Rh/Al_2O_3, and rhodium single crystal. The mode of adsorbed NO on Rh catalysts at room temperature has been found to strongly depend on the type of support and Rh dispersion. NO adsorption produced $Rh–NO^{\delta+}$ at 1920 cm^{-1}, neutral NO at 1838 cm^{-1}, gem-dinitrosyl NO at 1860 and 1780 cm^{-1}, and $Rh–NO^{\delta-}$ at 1740 and 1660 cm^{-1} on 5 wt% Rh/Al_2O_3 [12] and $Rh–NO^{\delta+}$ at 1921 cm^{-1} and $Rh–NO^{\delta-}$ at 1746 and 1656 cm^{-1} on 4 wt% Rh/SiO_2 [9]. It should be noted that the whole $Rh–NO^{\delta-}$ entity should be considered to be neutral. $\delta-$ represents the partial charge resulting from the transfer of electrons from Rh to NO. The difference in the wavenumber for $Rh–NO^{\delta-}$ at 1746 and 1656 cm^{-1} has been attributed to the different extent of electron back donation from the reduced Rh site to adsorbed NO. The bonding between Rh and $NO^{\delta-}$ at 1656 cm^{-1} (i.e., the low wavenumber $Rh–NO^{\delta-}$) is presumably

Table 1
Vibrational frequencies (cm^{-1}) of NO on Rh catalysts

	$Rh–NO^{\delta+}$	Rh–NO	$Rh(NO)_2$	$Rh–NO^{\delta-}$	Rh_2NO	Ref.
1.2 wt% Rh/Al_2O_3	1910–1920		$1830_{(as)}$ $1740–1744_{(s)}$			[11]
5.0 wt% Rh/Al_2O_3	1920	1838	$1860_{(as)}$ $1770_{(s)}$	1740 (high) 1660 (low)		[12]
0.5 wt% Rh/SiO_2		1855		1723–1740 (high) 1634–1680 (low)		This study
4.0 wt% Rh/SiO_2	1921			1740–1770 (high) 1650–1700 (low)		[9]
4.6 wt% Rh/SiO_2		1800		1685 (high) 1630 (low)		[13]
5.0 wt% Rh/SiO_2	1910	1830		1630–1690		[14]
Rh(111)		1840		1620–1644	1510–1570	[15,16]

stronger than that for Rh and $NO^{\delta-}$ at 1746 cm^{-1} (the high wavenumber Rh–$NO^{\delta-}$).

Our recent temperature-programmed reduction (TPR) and transient studies have revealed that the high wavenumber Rh–$NO^{\delta-}$ at 1746 cm^{-1} is less stable than the low wavenumber Rh–$NO^{\delta-}$ at 1656 cm^{-1} [17]; the low wavenumber $NO^{\delta-}$ participated in NO dissociation during NO–CO reaction on 4 wt% Rh/SiO_2 with the average Rh crystallite size of 63 Å at temperatures above 473 K [10]. The presence of both low and high wavenumber Rh–$NO^{\delta-}$ on the 4 wt% Rh/SiO_2 and the absence of the low wavenumber $NO^{\delta-}$ on 0.5 wt% Rh/SiO_2 suggest that the low wavenumber Rh–$NO^{\delta-}$ is chemisorbed on the surface of large Rh crystallites. The high wavenumber Rh–$NO^{\delta-}$ appeared to be chemisorbed on the surface of highly dispersed Rh on 0.5 wt% Rh/SiO_2. A high dispersion of Rh on 0.5 wt% Rh/SiO_2 is also evidenced by the fact that 0.5 wt% Rh/SiO_2 chemisorbed primarily linear CO as shown in Fig. 3.

EELS (Electron Energy Loss Spectroscopy) studies have shown that the surface of Rh(111) single crystal chemisorbs the low wavenumber Rh–$NO^{\delta-}$ at 1620–1644 cm^{-1} and 1510–1570 cm^{-1} which have been assigned to a bent terminal NO and a bridged NO, respectively [15,16]. The low wavenumber (1620–1644 cm^{-1}) Rh–$NO^{\delta-}$ observed on both Rh single crystal and supported Rh is in a bent form, exhibiting a Rh–N–O angle of 120° [18]. Both Rh–$NO^{\delta+}$ and Rh–NO on Rh/Al_2O_3 and Rh/SiO_2 are in a linear form which is perpendicular to the Rh surface. Rh–$NO^{\delta+}$ has only been observed on the supported Rh while bridged NO has only been found on the single crystal surface. The formation of $Rh-NO^{\delta+}$ on Rh/SiO_2 and Rh/Al_2O_3 is a result of either oxidation of the Rh surface by dissociative adsorption of NO or direct adsorption of NO on Rh^+ sites. The resistance of the Rh single crystal surface to oxidation during dissociative NO adsorption inhibits the formation of Rh^+ sites that chemisorb $NO^{\delta+}$ and gem-dicarbonyl.

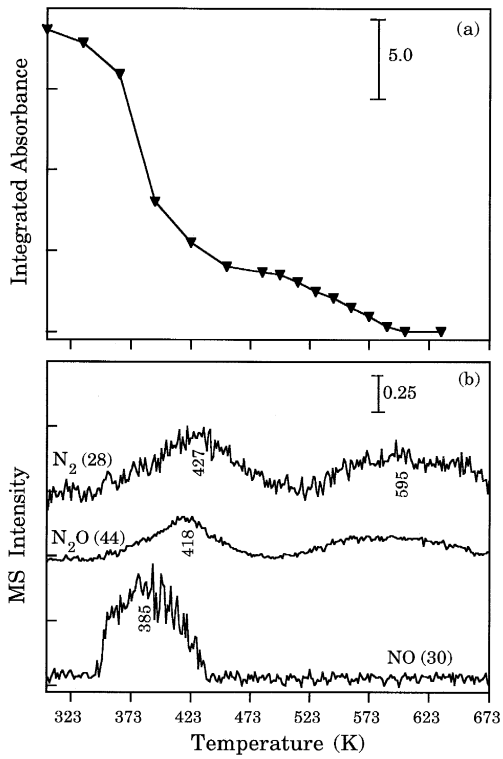

Fig. 2. (a) Variation of integrated absorbance between 1795 and 1460 cm^{-1} for Rh–$NO^{\delta-}$ band with temperature. (b) MS analysis of the effluent from the reactor for Fig. 1. Heating rate = 15 K min^{-1}. He = 30 cm^3 min^{-1}.

The variation in the integrated intensity of the high wavenumber Rh–$NO^{\delta-}$ at 1723–1740 cm^{-1} as a function of temperature is shown in Fig. 2(a); the variation in the composition of the IR cell effluent is shown in Fig. 2(b). The rapid decrease in IR intensity of Rh–$NO^{\delta-}$ in the 343–393 K temperature range corresponds to the desorption of adsorbed NO as gaseous NO and initial formation of N_2 and N_2O, suggesting the high wavenumber Rh–$NO^{\delta-}$ is responsible for the formation of N_2 and N_2O. Nevertheless, the extensive overlapping between 1723 and 1740 cm^{-1} does not allow determination of their contribution to the product formation. The first N_2 peak centered at 427 K corresponds to 0.69 μmol of N_2; the N_2O peak centered at 418 K correspond to 0.0053 μmol of N_2O. The

following reaction steps have been suggested to explain the formation of N_2 and N_2O products.

(a) $Rh^0 - NO^{\delta-} \rightarrow Rh^0 - N + Rh - O$

(b) $Rh^0 - N + Rh^0 - N \rightarrow N_2 + Rh^0$

(c) $Rh^0 - NO^{\delta-} + Rh - N \rightarrow N_2 + Rh - O + Rh$

(d) $Rh^0 - NO^{\delta-} + Rh^0 - N \rightarrow N_2O + 2Rh^0$.

Steps (a) and (d) leading to N_2O formation have been supported by ample evidence. Our recent pulse infrared study has shown that the low wavenumber Rh–$NO^{\delta-}$ in step (a) dissociates on the reduced Rh surface and the formation of N_2O takes place on the reduced Rh sites [10]. Fig. 1 also shows that a significant amount of N_2O was produced when the reduced Rh catalyst was exposed to NO. The formation of N_2O from adsorbed NO via steps (a) and (d) should leave an adsorbed oxygen which may modify the Rh surface. On 4 wt% Rh/SiO_2 and 5 wt% Rh/Al_2O_3 dissociative adsorption of NO, step (a), produced Rh^+ that chemisorbed NO as Rh–$NO^{\delta+}$. The absence of Rh–$NO^{\delta+}$ during NO adsorption and TPD indicates that Rh on 0.5 wt% Rh/SiO_2 is not oxidized.

It should be noted that the low wavenumber Rh–$NO^{\delta-}$ is not present during TPD. Formation of N_2O and N_2 during TPD should be attributed to dissociation of high wavenumber Rh–$NO^{\delta-}$, $Rh^0 - NO^{\delta-} \rightarrow Rh - N + Rh - O$. Adsorbed N and NO may follow steps (b) and (c) to produce a high temperature N_2 peak at 595 K and a low temperature N_2 peak at 427 K, respectively. Step (c) is supported by the presence of adsorbed NO during the formation of N_2 at 427 K. The slightly lower peak temperature for N_2O than for N_2 at 427 K indicates that step (d) takes place at a slightly lower temperature than step (c). Dissociation of the high wavenumber Rh–$NO^{\delta-}$ is not a common rate-determining step for the formation of N_2 and N_2O. Simulation of TPD profiles for adsorbed NO have revealed that both steps (c) and (d) have the same activation energy on a 5 wt% Rh/SiO_2 [19]. The factors that direct the reaction selectivity toward either step (c) or step (d) remain to be investigated.

The absence of an O_2 profile in Fig. 2 is consistent with the literature in that the oxygen produced from NO decomposition was not readily desorbed below 723 K [15,19,20]. During NO TPD, the O_2 desorption peak occurred at 1,500 K on Rh(111) [15], 1060 K on 5% Rh/SiO_2 catalyst [19], and 1,100 K on Rh filament [20].

The infrared spectra and gaseous composition profile shown in Figs. 1 and 2(b) permit the determination of the integrated absorbance coefficient ($\bar{A}_{NO}$ for Rh–$NO^{\delta-}$ by assuming that $\bar{A}_{NO}$ does not vary with the coverage of adsorbed NO and using the relation [21]

$$\bar{A}_{\mathrm{NO}} = \frac{1}{\bar{C}_{\mathrm{NO}}} \int_{\upsilon_1}^{\upsilon_2} A(\upsilon)\,\mathrm{d}\upsilon$$

where $\bar{C}_{\mathrm{NO}}$ is the moles of NO chemisorbed per cross sectional area of the catalyst disk. $A(\upsilon)$ is the adsorbate's absorbance which is the function of wavenumber υ, and υ_2 and υ_1 are the upper and lower wavenumber bounds at 1795 and 1640 cm^{-1}, respectively. The amount of NO adsorbed on the 0.5 wt% Rh/SiO_2 catalyst prior to TPD was determined by summing up all the nitrogen containing species obtained from multiplying the area under the TPD profile for each species by its responding factor. The amount of NO adsorbed on 196 mg of the catalyst was calculated to be 154.55 μl, which corresponds to an atomic dispersion based on a conservative estimation. $\bar{A}_{\mathrm{NO}}$ for Rh–$NO^{\delta-}$ is determined to be 1.91 $cm/\mu mol$.

Fig. 3 shows the IR spectra of adsorbed CO on 0.5 wt% Rh/SiO_2 at 303 K. Pulsing 25 μl of gaseous CO into helium flow did not produce adsorbed CO, indicating that CO adsorption is a slow process. Exposure of the catalyst to gaseous CO in a batch mode produced an intense band for the linear CO at 2049 cm^{-1}, a shoulder band at 2004 cm^{-1}, and bridged CO bands at 1813 and 1761 cm^{-1} at 303 K. The CO species

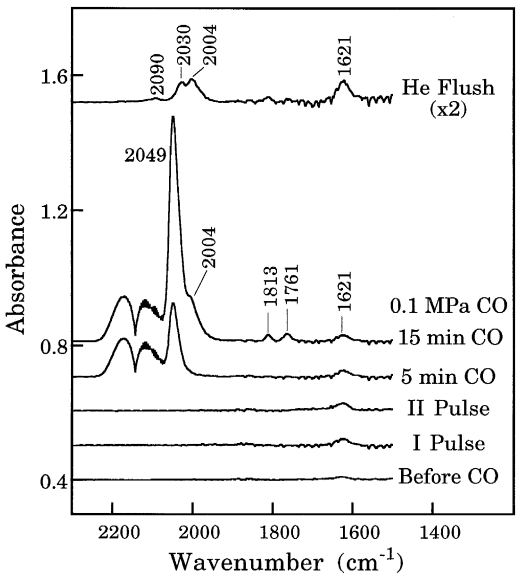

Fig. 3. IR spectra of CO adsorption on 0.5 wt% Rh/SiO_2 at 303 K.

exhibiting these bands are weakly adsorbed on the surface. These species can be easily removed by flowing helium, leaving weak bands at 2030 and 2004 cm^{-1} which may be assigned to $Rh(CO)_4$ [21]. It is unclear whether $Rh(CO)_4$ is produced from either the direct adsorption of CO on Rh or transformation from linear CO. A significant fraction of the 2030 cm^{-1} band can be assigned to linear CO on Rh^0 sites while a small fraction of the 2030 cm^{-1} and the 2090 cm^{-1} bands can be assigned to gem-dicarbonyl, $Rh^+(CO)_2$. In situ infrared study has shown that the formation of gem-dicarbonyl involve the reaction

$$\frac{1}{x}Rh_x^0 + OH(a) + 2CO_{(g)} \rightleftharpoons Rh^+(CO)_2 + \frac{1}{2}H_2$$

with OH(a) is the isolated OH on the surface of oxide support [3]. The reaction leading to the formation of gem-dicarbonyl is more facile on highly dispersed Rh/Al_2O_3 than on Rh/SiO_2. The reaction process can be reversed upon treatment of gem-dicarbonyl with H_2 above 200 K. The low intensity of gem-dicarbonyl on 0.5 wt% Rh/SiO_2 can be attributed to the depletion of surface OH by reduction the catalyst with H_2 at 673 K.

Fig. 4 shows the IR spectra of adsorbates as a function of temperature during the temperature-programmed reaction (TPR) under an NO–CO–He (NO:CO:He = 1:1:3) on Rh/SiO_2 catalyst. The initial spectrum prior to the NO–CO TPR shows a Rh–NO band at 1855 cm^{-1}, a Rh–$NO^{\delta-}$ band at 1723 cm^{-1}, and two shoulder bands at 1680 and 1634 cm^{-1}. These shoulder bands are assigned to the low wavenumber Rh–$NO^{\delta-}$ on the reduced Rh. Comparison of initial infrared spectra of adsorbed NO during TPD in Fig. 1 and during TPR in Fig. 4 shows that (i) the presence of CO in TPR results in the formation of adsorbed NO at 1634 and 1680 cm^{-1}, indicating that CO kept Rh in a reduced state and (ii) the presence of CO inhibits the reaction to produce N_2O.

Fig. 5(a) highlights changes in the IR intensity of adsorbed NO at 1723 cm^{-1} with respect to temperature; Fig. 5(b) shows variation in the composition of the IR cell effluent during TPR. Increasing the temperature from 303 to 453 K led to a gradual decrease in the intensity of

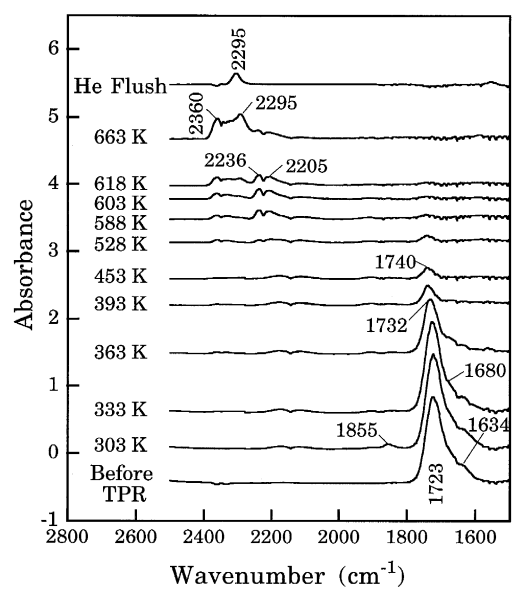

Fig. 4. IR spectra during the temperature-programmed reaction of NO–CO–He (1:1:3) on Rh/SiO_2. Heating rate = 15 K min^{-1}. He = 30 cm^3 min^{-1}.

adsorbed NO while conversion of reactants to products is negligible, indicating desorption of adsorbed NO. An appreciable conversion of reactants was observed at temperatures above 475 K where the high wavenumber Rh–$NO^{\delta-}$ band shifted to 1740 cm^{-1}. The light-off temperature, at which 50% conversion occurs, was observed at 587 K, where the intensity of adsorbed NO is about 2% of its initial intensity at 303 K. The light-off temperature under the same reaction condition on 4 wt% Rh/SiO_2 was determined to be 530 K [17]. The major IR-observable products at the light-off temperature are CO_2 and N_2O as shown by their intense IR bands. Because both N_2O and CO_2 give $m/e = 44$, the quantitative analysis of these species is not possible with MS without monitoring the secondary ionization of CO_2, $m/e = 22$.

Nearly complete conversion of NO was achieved at temperatures above 663 K where the only noticeable adsorbate band was Si–NCO at 2295 cm^{-1}. The Si–NCO band first appeared at 588 K and became prominent at 663 K. Si–NCO has been known to be a spectator species for CO_2 formation which remains on the catalyst surface under flowing helium at temperature between 463–723 K [10,22]. The absence of adsorbed NO and CO at temperatures above 618 K indicates that the concentration of these adsorbates is too small to be detected by IR.

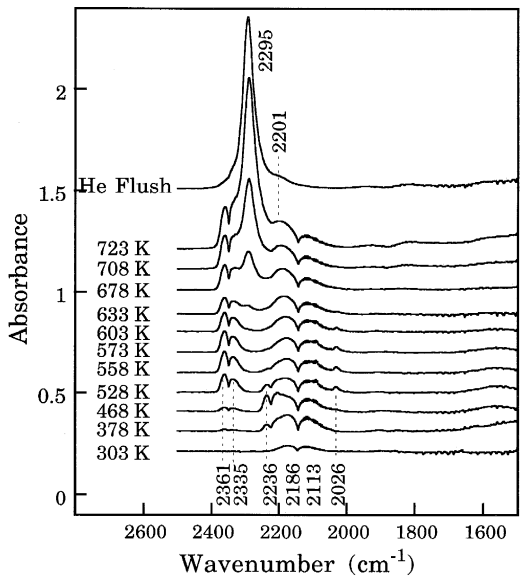

Fig. 6. IR spectra during the temperature-programmed reaction of NO–CO–He (1:10:6) on Rh/SiO_2. Heating rate = 15 K min^{-1}. He = 30 cm^3 min^{-1}.

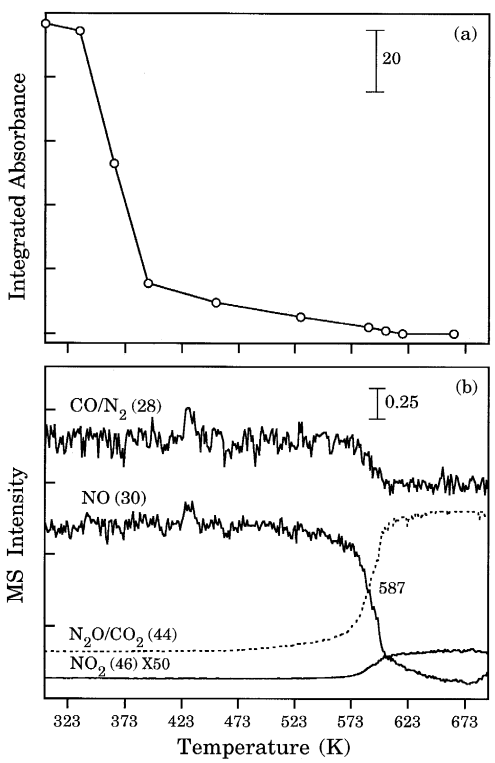

Fig. 5. (a) Variation of integrated absorbance between 1795 and 1460 cm^{-1} for Rh–$NO^{\delta-}$ band with temperature. (b) MS analysis of the effluent from the reactor for Fig. 4.

In order to observe adsorbed CO during TPR, the ratio of NO to CO was adjusted to 1:10 to increase the concentration of adsorbed CO. Fig. 6 shows the IR spectra of the adsorbates. The reason of the absence of CO adsorbate at 303 K is not clear. Fig. 7 exhibits the composition profile of the IR cell effluent as a function of temperature during TPR with NO:CO:He = 1:10:6. N_2O and CO_2 bands emerged at 378 K. Formation of N_2O and CO_2 occurred at significantly lower temperatures than those of the TPR study with NO:CO:He = 1:1:3. Fig. 7 shows that $m/e = 44$ starts to increase in intensity at 378 K, confirming the formation of N_2O and

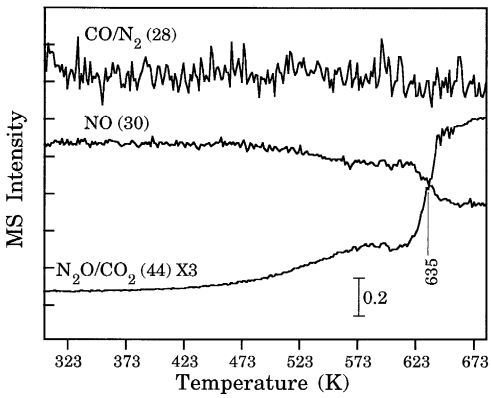

Fig. 7. MS analysis of the effluent from the reactor for Fig. 6.

CO_2. Formation of N_2O from NO–CO reaction has been shown to occur on the reduced Rh surface [10]. The high concentration of CO appears to keep a portion of the Rh in the reduced form, enhancing the formation of N_2O and CO_2. The presence of reduced Rh site is also evidenced by the linear CO band at 2026 cm^{-1} which emerged at 468 K.

The light-off of the reaction took place at 635 K where Rh–NCO at 2201 cm^{-1} and Si–NCO at 2295 cm^{-1} began to appear. Si–NCO is formed by spillover of isocyanates from the rhodium surface onto the support [10,22]. The high concentration of CO favors the formation of both Rh–NCO and Si–NCO. By varying the partial pressure of CO and NO on 5 wt% Rh/SiO_2, it was also found that an increase in the partial pressure of CO led to an increase in the Rh–NCO intensity and a decrease in the $Rh–NO^{\delta-}$ intensity [23].

A comparison of the behavior of adsorbed NO and CO on 0.5 wt% Rh/SiO_2 and 4 wt% Rh/SiO_2 shows that the different dispersion of Rh crystallite leads to distinct differences in chemisorptive and reactivity properties [8–10]. Both linear and bridged CO are weakly bonded to the surface of the highly dispersed Rh, but strongly bonded to the surface of large Rh crystallites. During the TPR of NO–CO (1:1) reaction, the high wavenumber $Rh–NO^{\delta-}$ is the dominant adsorbate on 0.5 wt% Rh/SiO_2 while gem-dicarbonyl and both low and high wavenumber $Rh–NO^{\delta-}$ are present below the light-off temperature and linear CO is the major adsorbate above the light-off temperature on 4 wt% Rh/SiO_2. 4 wt% Rh/SiO_2 shows higher activity for NO–CO reaction with a lower light-off temperature than 0.5 wt% Rh/SiO_2. The high light-off temperature for 0.5 wt% Rh/SiO_2 may be related to its high wavenumber $Rh–NO^{\delta-}$ which has less propensity for dissociation than the low wavenumber $Rh–NO^{\delta-}$.

4. Conclusions

The 0.5 wt% Rh/SiO_2 gives highly dispersed Rh which chemisorbs NO as the high wavenumber $Rh–NO^{\delta-}$ at 1740–1723 cm^{-1} and chemisorbs CO as linear, bridged, and $Rh(CO)_4$. The bonding for $Rh–NO^{\delta-}$ is significantly stronger than that for Rh–CO. During TPD of $Rh–NO^{\delta-}$, adsorbed NO decomposed to N_2 as a major product and N_2O as a minor product. The NO–CO TPR shows that CO reduces a portion of the Rh sites, promoting the formation of N_2O at 378 K. For the TPR, increasing CO partial pressure from NO:CO:He = 1:1:3 to NO:CO:He = 1:10:6 caused a progressive increase in NO conversion and a significant increase in Rh–NCO and Si–NCO concentration. Results of this study and previous studies on 4 wt% Rh/SiO_2 show that differences in Rh dispersion can lead to significant variation in chemisorptive properties and reactivity of the Rh surface. A systematic understanding of the effect of dispersion on the nature of adsorption sites and reactivity remains to be investigated.

Acknowledgements

The authors gratefully acknowledge partially financial support of this research from the U.S. Department of Energy (grant number DE-FG22-95PC95224).

References

[1] Y.E. Li and R.D. Gonzalez, J. Phys. Chem., 92 (1988) 1589.
[2] W. Delgass, G. Haller, R. Kellerman and J. Lunsford, Spectroscopy in Heterogeneous Catalysis, Academic Press, New York, 1979.
[3] P. Basu, D. Panayotov, and J. T. Yates, J.r., J. Am. Chem. Soc., 110 (1988) 2074.
[4] J.T. Yates, Jr. and T.E. Madey (Editors), Vibrational Spectroscopy of Molecules on Surfaces, Plenum Press, New York, 1987.
[5] K. Tamaru, in J. Anderson and M. Boudart (Editors), Catalysis: Science and Technology, Vol. 9, Springer Verlag, Berlin/Heidelberg/New York, 1991, p. 87.
[6] S.I. Pien and S.S.C. Chuang, J. Mol. Catal., 68 (1991) 313.
[7] S.S.C. Chuang and S.I. Pien, J. Catal., 135 (1992) 618.
[8] S.S.C. Chuang, M. A. Brundage, M. W. Balakos and G. Srinivas, Appl. Spec. 49(8) (1995) 1151.
[9] G. Srinivas, S.S.C. Chuang and S. Debnath, J. Catal., 148 (1994) 748.
[10] R. Krishnamurthy and S.S.C. Chuang, J. Phys. Chem., 99 (1995) 16727.
[11] E.A. Hyde, R. Rudham and C.H. Rochester, J. Chem. Soc., Faraday Trans. 1, 80 (1984) 531.
[12] S. Solymosi, T. Bansagi and E. Novak, J. Catal., 112 (1988) 183.
[13] W.C. Hecker and A.T. Bell, J. Catal., 84 (1983) 200.
[14] B.J. Savatsky and A.T. Bell, ACS Symp. Ser., 178 (1982) 105.
[15] T.W. Root, G.B Fisher and L.D Schmidt, J. Chem. Phys., 85(8) (1986) 4679.
[16] G.B. Fisher, C.L. DiMaggio and D.D. Beck, in L. Guczi, F. Solymosi and P. Tetenyi (Editors), Proceedings of the 10th International Congress on Catalysis, 19–24 July, 1992, Part A, Elsevier, Amsterdam, 1992, p. 383.
[17] S.S.C. Chuang, R. Krishnamurthy and G. Srinivas, in U.S. Ozkan, S.K. Agarwal and G. Marcelin (Editors), Reduction of Nitrogen Oxide Emissions, ACS Symposium, Vol. 587, Am. Chem. Soc., Washington, DC, 1995, Chap. 14, p. 183.
[18] N.J. Connelly, Inorg. Chim. Acta, 6 (1972) 47.
[19] A.A. Chin and A.T. Bell, J. Phys. Chem., 87 (1983) 3700.
[20] B.E. Nieuwenhuys, in R.W. Joyner and R.A. van Santen (Editors), Elementary Reaction Steps in Heterogeneous Catalysis, Kluwer Academic Publishers, Dordrecht, Netherlands, 1993, p. 155.
[21] S.S.C. Chuang, R. Krishnamurthy and C.D. Tan, Coll. and Surf. A: Physicochemical and Eng. Aspects, 105 (1995) 35.
[22] G. Srinivas, S.S.C. Chuang and S. Debnath, in J.N. Armor (Editor), Environmental Catalysis, ACS Symposium Series, Vol. 552, Am. Chem. Soc., Washington, DC, 1994, Chap. 12, p. 158.
[23] W.C. Hecker and A.T. Bell, J. Catal., 85 (1984) 389.